How Internally Coupled Ears Generate Temporal and Amplitude Cues for Sound Localization

A. P. Vedurmudi,[1] J. Goulet,[1,2] J. Christensen-Dalsgaard,[3] B. A. Young,[4] R. Williams,[4] and J. L. van Hemmen[1]
[1]Physik Department T35 & Bernstein Center for Computational Neuroscience–Munich, Technische Universität München, 85747 Garching bei München, Germany
[2]Institute of Neuroscience and Medicine - Neuromodulation INM-7, Research Center Jülich, 52425 Jülich, Germany
[3]Center for Sound Communication, Syddansk Universitet, Campusvej 55, 5230 Odense M, Denmark
[4]Kirksville College of Osteopathic Medicine, A.T. Still University, Kirksville, Missouri 63501, USA
(Received 21 May 2015; revised manuscript received 23 August 2015; published 14 January 2016)

In internally coupled ears, displacement of one eardrum creates pressure waves that propagate through air-filled passages in the skull and cause displacement of the opposing eardrum, and conversely. By modeling the membrane, passages, and propagating pressure waves, we show that internally coupled ears generate unique amplitude and temporal cues for sound localization. The magnitudes of both these cues are directionally dependent. The tympanic fundamental frequency segregates a low-frequency regime with constant time-difference magnification from a high-frequency domain with considerable amplitude magnification.

DOI: 10.1103/PhysRevLett.116.028101

Internally coupled ears (ICE), in which the two tympanic membranes (eardrums) are functionally coupled by an air-filled passage through the skull, occur in most frogs, lizards, alligators, and birds, conservatively, more than 15 000 species. In this auditory system the eardrums are driven by a combination of external sound pressure and internal cavity pressure resulting from the vibration of the opposite eardrums [1–3]. If the interaural distance L between the eardrums is small, the time difference between excitation of the opposing membranes due to an external pressure is too small for effective neuronal processing, precluding sound localization using temporal cues. Furthermore, for most vertebrates, the interaural level (or intensity) difference is negligible, whatever the source direction. With ICE, however, an animal can amplify the time differences as well as generate considerable (e.g., ≤ 20 dB) direction-dependent amplitude differences between the eardrum vibrations. Thus ICE enables even animals with a small interaural distance to localize sound sources.

An earlier analytical paper [2] was formulated to explain data gathered from a few species of Gekkonid lizards [1]. In contrast, we present here a general model of ICE, which has been formulated with four goals. First, to be applicable to the full range of anatomical variation, relative to both head and tympanum size, observed in animals with ICE. Second, one of the main anatomical variations among the species with ICE is the diameter of the coupling passageway; the model incorporates this (Fig. 1). Third, while not neglecting the pressure-wave's dependence upon the specific geometry, our emphasis is on the sensory cues arising from the dynamical patterns of tympanic displacements. In so doing we account for a uniform plateau, whatever the direction θ, in the fraction of internal and interaural time differences, the so-called time expansion factor, for lower frequencies (typically, < 0.7 kHz) as well as the amplitude amplification at much higher frequencies (say, around 1.3 kHz). Fourth, the proffered model relates both the temporal and intensity domains through the fundamental frequency f_0 of the tympanic membrane, which acts as the transformer between the external auditory stimuli and the internal sound processing.

Previous studies [4,5] found that lizards have two discrete populations of cochlear hair cells, one that responds to amplitude cues and the other to temporal cues. These two hair-cell populations both project (ultimately) bilaterally, giving the organism a neuronal template to contrast the amplitude and temporal patterns arising from the tympana. We are following Jørgensen *et al.* [6] in postulating an algorithm for determining amplitude (level) differences, more specifically, a neuronal subtraction of logarithmic vibration amplitudes of the two membranes. The biological physics is that of hair-cell response being governed by the (Weber-Fechner) logarithm of the amplitude whereas the "subtraction" is that of excitation minus inhibition (E/I) and is a nonliteral criterion. We refer to this subtraction as the internal level difference (iLD) and contrast it with the interaural level difference (ILD), i.e., the logarithmic amplitude difference between the *external* sound inputs to both ears. It is also known that certain neurons are sensitive to time differences between eardrum vibrations [7–9]. We refer to this metric as the internal time difference (iTD), in contrast to the interaural time difference (ITD). Herein we demonstrate how iTDs and iLDs emerge solely due to the internal acoustic coupling between the eardrums.

The model presented herein is *universal* in the sense that, with an appropriate change in parameters, it is applicable

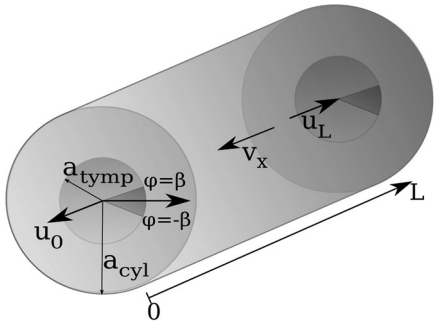

FIG. 1. Because of the coupling of the eardrums through the internal cavity, an animal equipped with ICE perceives internal rather than interaural time and level differences. The cavity is modeled as a cylinder of volume V_{cav} and length L (radius $a_{\mathrm{cav}} = \sqrt{V_{\mathrm{cav}}/\pi L}$). The bold arrows indicate our direction conventions along the x axis, and the smaller circles at either end indicate the eardrums with radius $a_{\mathrm{tymp}} \leq a_{\mathrm{cav}}$.

to all species with ICE. We model the internal cavity as an air-filled cylinder of length L based on typical head sizes observed in Nature. We fix the cavity volume V_{cav} and calculate the cylinder radius using $a_{\mathrm{cav}} = \sqrt{V_{\mathrm{cav}}/\pi L}$. The three-dimensional model for the cavity is illustrated in Fig. 1. The smaller circles at either end of the cylinder correspond to the eardrums.

The inputs are modeled as plane waves of a certain wavelength of a pure tone incident on both ears. Since typical wavelengths are much larger than the membrane diameter, we can safely assume the incident pressure to be of uniform amplitude p_{ex},

$$p_0 = p_{\mathrm{ex}} e^{i\omega t} e^{ik\Delta/2}, \qquad p_L = p_{\mathrm{ex}} e^{i\omega t} e^{-ik\Delta/2}. \quad (1)$$

$\Delta = L \sin\theta$ is the differential distance between the sound source and the two ears with θ as the source direction with respect to the head's median axis; unless stated otherwise, $\theta = \pm 90°$. Furthermore, for the (external) interaural time difference, ITD $= \Delta/c$ with c as velocity of sound in air, while $\omega = 2\pi f$ is the angular frequency of an incident sound wave. Finally, the wave number is given by $k = \omega/c$.

At our frequencies of interest (< 4 kHz), viscous acoustic damping can be neglected so we follow common acoustic models [10–12] and describe the air inside the cavity using linear acoustics with cylindrical coordinates. In this approach, the air moves due to a local pressure $p(x, r, \phi; t)$ obeying the three-dimensional wave equation

$$\frac{1}{c^2}\frac{\partial^2 p(x,r,\phi;t)}{\partial t^2} = \Delta_{(2)} p(x,r,\phi;t) + \frac{\partial^2 p(x,r,\phi;t)}{\partial x^2},$$
$$\Delta_{(2)} = \frac{1}{r}\frac{\partial}{\partial r} + \frac{\partial^2}{\partial r^2} + \frac{1}{r^2}\frac{\partial^2}{\partial \phi^2}. \quad (2)$$

$\Delta_{(2)}$ is the two-dimensional Laplacian in polar coordinates. On the eardrum, the air velocity is related to p by [11]

$$-\rho \frac{\partial \mathbf{v}}{\partial t} = \nabla p. \quad (3)$$

We require both that p be continuous and smooth in ϕ, and that the normal velocity vanishes at the borders [10]: $v_r|_{r=a_{\mathrm{cav}}} = 0$. Separating variables, we obtain a specific solution for frequency $f = \omega/2\pi$ and with spatial part

$$p_{qs}(x,r,\phi) = (A_{qs} e^{i\zeta_{qs}x} + B_{qs} e^{-i\zeta_{qs}x}) f_{qs}(r,\phi),$$
$$f_{qs}(r,\phi) = J_q(\nu_{qs} r/a_{\mathrm{cav}})(C_{qs}\cos q\phi + D_{qs}\sin q\phi). \quad (4)$$

J_q is the order-q ($q = 0, 1, 2, \ldots$) Bessel function of the first kind and ν_{qs} the sth positive zero of J'_q. The wave number in the x direction is given by $\zeta_{qs} = (k^2 - \nu_{qs}^2/a_{\mathrm{cav}}^2)^{1/2}$. The f_{qs} are an orthogonal set of functions when integrated over a disk of radius a_{cav}. The general solution is given by a linear combination of $p_{qs}(x,r,\phi)e^{\pm i\omega t}$.

In order to determine A_{qs} and B_{qs} we need an expression for the membrane vibrations. In vertebrates, the membrane's inner surface is bound to a cartilage or bony element of the middle ear (commonly, the extracolumella); this attachment is typically asymmetrical and places a significant mechanical load on the membrane [13].

We therefore consider the eardrum as a sectorial membrane rigidly clamped between angles $\phi = \pm\beta$, meaning that its vibrating part is limited to a circular sector between $\beta < \phi < 2\pi - \beta$ with vanishing amplitude between $\phi = \pm\beta$; cf. Fig. 1. The extracolumella is effectively of infinite mass and motionless, a reasonable approximation since the extracolumella and attached proximal elements are typically (300×) heavier than the rest of the membrane.

Finally, the radius a_{tymp} of the equivalent *circular* membrane is calculated from the area of a realistic eardrum of surface A through $a_{\mathrm{tymp}} = \sqrt{A/\pi}$.

The eardrum is modeled as a damped linear-elastic membrane obeying

$$-\frac{\partial^2 u}{\partial t^2} - 2\alpha\frac{\partial u}{\partial t} + c_M^2 \Delta_{(2)} u = \frac{1}{\rho_m d}\Psi(r,\phi;t) \quad (5)$$

with displacement $u(r,\phi;t)$, damping coefficient α, density ρ_m, thickness d, and wave-propagation velocity $c_M = \sqrt{T_0/\rho_m}$ where T_0 is the membrane tension. Furthermore, $\Psi(r,\phi;t)$ is the total pressure driving the membrane, which is fixed at its radial boundary, $r = a_{\mathrm{tymp}}$ and, due to the extracolumella, at $\phi = \pm\beta$.

The membrane eigenmodes are found by first solving (5) in the free, undamped case, i.e., for $\Psi = 0$ and $\alpha = 0$. We substitute

$$u_{\mathrm{mn}}^{\pm}(r,\phi;t) = g_{\mathrm{mn}}(r,\phi) e^{\pm i\omega_{\mathrm{mn}} t}, \quad (6)$$

$$g_{\mathrm{mn}}(r,\phi) = \sin\kappa(\phi - \beta) J_\kappa(\mu_{\mathrm{mn}} r), \quad (7)$$

where $\kappa[m] = m\pi/2(\pi - \beta)$ ($m \geq 1$) and J_κ is the order-κ Bessel function of the first kind; $\mu_{\mathrm{mn}} a_{\mathrm{tymp}}$, is its nth zero,

and $\omega_{mn} = c_M \mu_{mn}$ is the corresponding eigenfrequency. The g_{mn} are an orthogonal set of functions when integrated over the membrane disk $\{r \le a_{tymp}, \beta \le \phi \le 2\pi - \beta\}$.

We consider the case where the membrane is driven by a uniform pressure, i.e., $\Psi(r,\phi,t) = p_{ex} e^{i\omega t}$. In the quasistationary state, the forced membrane vibrates with a frequency equal to that of the input. The solution is found by substituting a linear combination of $g_{mn}(r,\phi)e^{\pm i\omega t}$ into

$$\sum_{m=1,n=1}^{\infty} \Omega_{mn} C_{mn} g_{mn}(r,\phi) e^{i\omega t} = p_{ex} e^{i\omega t}, \tag{8}$$

where $\Omega_{mn} = \rho_m d[(\omega^2 - \omega_{mn}^2) - 2i\alpha\omega]$. The C_{mn} can be calculated through the membrane mode orthogonality.

In ICE, the coupled membranes are driven by *both* the external pressure (1) *and* the internal pressure (2). Substitution of linear combinations of g_{mn} and the internal pressure $p(x,r,\phi)e^{i\omega t}$ as a linear combination of the pressure modes (4) into (5) gives

$$\sum_{m,n}^{\infty} \Omega_{mn} C_{mn}^{0/L} g_{mn} = p_{0/L} - p(0/L,r,\phi), \tag{9}$$

$$u_{0/L}(r,\phi;t) = \sum_{m=0,n=1}^{\infty} C_{mn}^{0/L} g_{mn}(r,\phi) e^{i\omega t}, \tag{10}$$

where $(x=)0$ and $(x=)L$ denote the ends of the cylinder. We have also canceled the time-dependent terms in (9).

Because of the no-penetration condition, we equate the air velocity (3) to that of the surface composed of the eardrum and the remaining cylinder base $a_{tymp} < r < a_{cav}$. This velocity is nonzero on the vibrating membrane and zero on the extracolumella and remaining cylinder base; cf. Fig. 1, indicating the context of the above boundary condition. In our convention, velocities along the x axis out of the cylinder are taken to be positive.

We now face the problem that the membrane and cavity modes are not mutually orthogonal. In other words, each membrane mode couples with every cavity mode. We circumvent this problem by approximating [14] the boundary conditions for (2) and (3) in that we effectively replace each membrane by a circular piston operating on the internal pressure p and moving with the membrane's average velocity $\dot{u}_{0/L}^{ave}$ so that

$$u_{0/L}^{ave} = \frac{1}{\pi a_{cav}^2} \int \mathrm{d}S u_{0/L}, \qquad \dot{u}_{0/L}^{ave} = i\omega u_{0/L}^{ave}, \tag{11}$$

$$v_x(0,r,\phi) := -\dot{u}_0^{ave}, \qquad v_x(L,r,\phi) := \dot{u}_L^{ave}. \tag{12}$$

The second relation in (11) directly follows from (10). By doing so, we implicitly exploit the fact that typical vibration amplitudes for tympanic membranes are of the order of nanometers. We can therefore still use the same cavity eigenmodes as before. Furthermore, the higher cavity modes have eigenfrequencies that are in general well beyond (> 10 kHz) the typical lizard's hearing range and will not play a significant role. The modal expansion of the air velocity is computed by substituting (4) in (3). This is the piston approximation as depicted in Fig. 2. A direct consequence of the piston approximation is that the higher pressure modes vanish and internal pressure is only composed of the 00 modes, corresponding to a standing wave along the x axis,

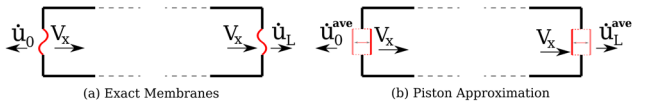

FIG. 2. Left: exact membrane boundary conditions. The velocity of air (v_x) equals that of the membrane ($\dot{u}_{0/L}$). Right: piston approximation. The membrane is approximated by a circular piston moving with the membrane's average velocity and with boundary conditions (12) applied to (2) and (3). The piston approximation refers to (2) and the boundary condition for the pressure p in the three-dimensional cavity, not to the motion (5) of the eardrum itself.

$$p(x,r,\phi;t) = \frac{\rho\omega^2 L}{2kL\sin kL}[u_0^{ave}\cos k(L-x) + u_L^{ave}\cos kx]e^{i\omega t}.$$

Finally, by substituting this result into the membrane equation (5), we can calculate $u_{0/L}^{ave}$ as a function of the input direction and frequency,

$$\frac{2\rho c^2}{L} u_{0/L}^{ave} = \frac{p_L + p_0}{1/\Lambda + \Gamma_+} \mp \frac{p_L - p_0}{1/\Lambda + \Gamma_-}, \tag{13}$$

where

$$\Lambda = \frac{\rho c^2}{V_{cav}} \sum_{m,n}^{\infty} \frac{(\int g_{mn})^2}{\Omega_{mn} \int g_{mn}^2},$$
$$\Gamma_+ = -kL\cot kL/2, \qquad \Gamma_- = kL\tan kL/2, \tag{14}$$

so that $|\Lambda| \le (\rho c^2 \mathcal{S}/V_0)\sum_{m,n} 1/|\Omega_{m,n}| < \infty$ by Cauchy-Schwarz, with $\mathcal{S}$ as the tympanic area. Λ quantifies the frequency response of an uncoupled membrane whereas the $\Gamma_\pm$ result from the internal pressure. In order to calculate Λ we chose a cutoff of $N = 30$ modes. Higher modes are suppressed by the high damping at their corresponding eigenfrequencies.

In order to compare our model with experimental results, we define the average vibration velocity in dB re $\mathrm{mms^{-1}Pa^{-1}}$, meaning the decibel velocity in mm/s for an input pressure amplitude of 1 Pa as $v_{dB} = 20\log_{10}|\dot{u}_{0/L}^{ave}|$. Using parameters based on standard anatomical data (see Table I) and an extracolumellar angle $\beta = \pi/30$, we get membrane-vibration velocity $c_M = 5.4$ m/s for the Tokay gecko (*Gecko*) and $c_M = 2.9$ m/s for the water monitor (*Varanus*)—a rather different perspective.

TABLE I. System parameters: *Gecko* and *Varanus*

Parameter	*Gecko*	*Varanus*
Interaural distance L	22 mm	16 mm
Eardrum radius a_{tymp}	2.6 mm	2.6 mm
Membrane density ρ_m	1 mg/mm^3	1.2 mg/mm^3
Eardrum thickness d	10 μm	30 μm
Cavity volume V_{cav}	3.5 ml	2.0 ml
Fundamental frequency f_0	1.05 kHz	0.4 kHz
Damping coefficient α	$\approx 2611\text{s}^{-1}$	$\approx 350\text{s}^{-1}$

Before proceeding we turn to a few experimental checks of the general ICE theory. The price we pay for generality is that we do not delve into possible microstructures of the tympana. Figures 3(a) and 3(b) show the respective frequency dependence of the membrane vibrations for ipsilateral $\theta = 90°$ and contralateral $\theta = -90°$ stimuli for both *Gecko* and *Varanus*.

In the case of *Gecko*, the contralateral response has a minimum near f_0, whereas the spectral response of *Varanus* shows multiple peaks corresponding to higher membrane eigenfrequencies. The occurrence of multiple peaks instead of a single one in the biophysically relevant range is due to the fact that the *Varanus* eardrum is heavily underdamped [much smaller α; cf. Eq. (5)], resulting in higher modes being less suppressed. Nevertheless, our ICE model explains the frequency behavior in both cases.

In the following, we focus on three universal aspects of ICE: (1) The internal time difference (iTD), which for frequencies $< f_0$ greatly exceeds the interaural time difference (ITD); (2) the internal level difference (iLD), which exhibits a pronounced maximum once the iTD has strongly decreased; and (3) the segregation of the iTD and iLD domains by the fundamental frequency f_0 of the tympanum. Both iTD and iLD depend on the sound-source direction.

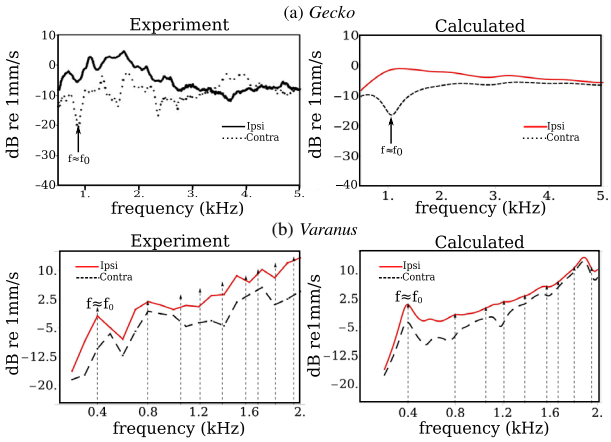

FIG. 3. Experimental and calculated v_{dB} for ipsi- ($\theta = 90°$) and contralateral ($\theta = -90°$) stimuli for *Gecko* (top) and *Varanus* (bottom). The flaccid membrane of *Varanus* (with low α) gives peaks at f_0 as well as at higher membrane resonances. As elsewhere, all membrane eigenfrequencies are indicated by vertical dashed lines; cf. Fig. 5(b). The first resonant peak (or trough) allows a straightforward determination of tympanic eigenfrequency f_0 in the alive animal. All experimental data presented were gathered by using laser Doppler vibrometry.

The internal time difference (iTD) corresponds to the actual time difference between left and right membrane vibrations as experienced by the animal,

$$\text{iTD} = \text{Arg}(\dot{u}_0^{\text{ave}}/\dot{u}_L^{\text{ave}})/\omega. \tag{15}$$

For *Gecko*, the interaural time difference (ITD) equals $\text{Arg}(p_0/p_L)/\omega = L\sin\theta/c$, the time taken by sound to travel across the head. It is independent of frequency and for our parameters it is ≈ 64 μs for $\theta = \pm 90°$. Figures 4(a) and 4(b) show the frequency and direction dependence of the iTDs for *Gecko* and *Varanus*, respectively. In the case of *Gecko*, the iTDs have a low-pass response; i.e., they are more or less constant up to a certain frequency and drop sharply thereafter, with iTD/ITD $= 1$ at $f \approx f_0$. From a neuronal-processing point of view, this is convenient as it mirrors the behavior of the ITDs *but is strongly increased* by a factor of about 3 [15]. The number 3 is not unique, rather the value depends on the specific geometry of the internal cavity. Figure 4(b) illustrates its variation.

Although the membrane vibration amplitudes are directional by themselves, the difference between left and right tympanum is more sensitive to θ. For the input (1), the internal level difference (iLD) is defined as the logarithmic difference between the left and right (0/L) membrane amplitudes of (8),

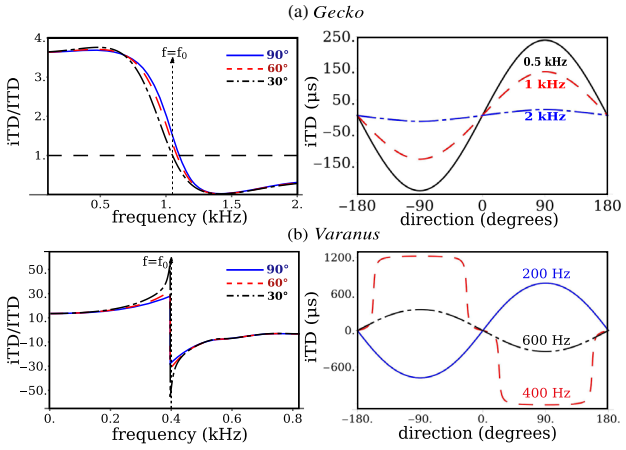

FIG. 4. Frequency and direction dependence of the iTDs for *Gecko* (top) and *Varanus* (bottom). (a) For *Gecko*, the iTDs exhibit a plateau of iTD ≈ 3 ITD up to about $f = f_0$ and sharply fall thereafter. As indicated, the plateau exists irrespectively of the direction θ; cf. left column. The iTDs can thus be effective low-frequency cues. (b) For *Varanus*, the iTDs slowly increase up to f_0 and then decrease; the discontinuity is an artifact of 2π. The young animal can therefore only exploit a restricted low-frequency range of iTDs up to, say, 200 Hz, nevertheless illustrating that the time expansion factor iTD/ITD can differ from 3 appreciably.

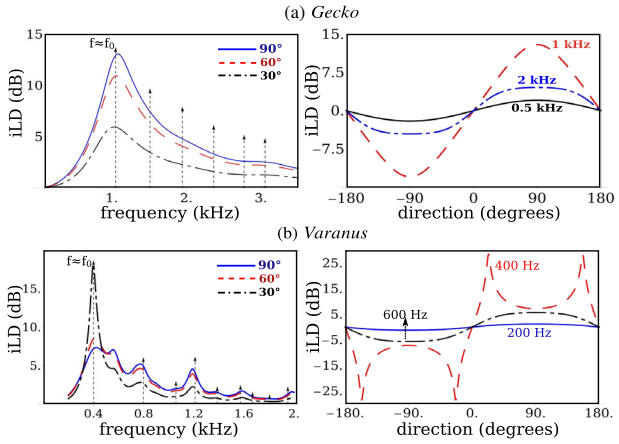

FIG. 5. Calculated frequency and direction dependence of the iLDs for *Gecko* (top) and *Varanus* (bottom). (a) For *Gecko*, the iLDs peak close to $f = f_0$ and decrease slowly thereafter. They can therefore serve both as effective high-frequency hearing cues and as an efficient means of determining f_0 in alive animals. Clearly, the higher tympanic eigenmodes play no role. (b) For juvenile *Varanus* with small α and $f_0 \approx 400$ Hz, we see corresponding peaks also at higher membrane eigenmodes.

$$\mathrm{iLD} = 20\,\mathrm{Log}_{10}|u_L^{\mathrm{ave}}/u_0^{\mathrm{ave}}| = 20\,\mathrm{Log}_{10}|\dot{u}_L^{\mathrm{ave}}/\dot{u}_0^{\mathrm{ave}}|,$$
$$u_L^{\mathrm{ave}}/u_0^{\mathrm{ave}} = (1+B)/(1-B) \tag{16}$$

where

$$B = i[(1+\Lambda\Gamma_+)/(1+\Lambda\Gamma_-)]\tan(k\Delta/2) \tag{17}$$

is direction dependent through $\Delta = L\sin\theta$. The $\Gamma_\pm$ in (17) stem from (14). Once left and right inputs effectively have the same amplitude, we can put the interaural level difference (ILD) equal to zero. For *Gecko*, the iLD has a bandpass-like behavior. It is zero for both very low and high frequencies and peaks close to the membrane eigenfrequency f_0; cf. Fig. 5(a). The iLDs steeply increase across $\theta = 0°$ and are at a maximum or minimum at $\theta = \pm 90°$. For *Varanus*, Fig. 5(b) shows an iLD spectrum with multiple peaks near membrane resonances, corresponding to a much lower damping (smaller α). Moreover, at the fundamental membrane eigenfrequency f_0, the directional response peaks at $\theta = \pm 30°$. A possible explanation of this deviating behavior is that the experiments were performed on juvenile monitor lizards, suggesting that increased membrane damping and cavity volume in adults should give similar results to those shown for the adult *Gecko*.

With ICE we have come across a hearing system that relies on iTDs at low frequencies and iLDs at higher frequencies, with the transition between the two regimes being governed by the fundamental eigenfrequency f_0 of the tympanic membrane; see Fig. 6. In this way the fundamental frequency of the eardrum creates a partition of the sensory landscape.

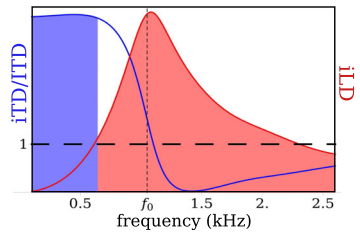

FIG. 6. Transition between the iTD and iLD frequency regime for directions $\theta \neq 0°$. At lower frequencies iTDs work better as directional cues, e.g., with $\mathrm{iTD}/\mathrm{iTD} \approx 3$ (blue plateau) for adult geckos, while at higher frequencies the iLD becomes pronounced, even though for most lizards the external $\mathrm{ILD} \approx 0$. The transition between the two kinds of cues is governed by the eardrum's fundamental frequency f_0.

[1] J. Christensen-Dalsgaard and G. A. Manley, J. Exp. Biol. **208**, 1209 (2005).
[2] C. Vossen, J. Christensen-Dalsgaard, and J. L. van Hemmen, J. Acoust. Soc. Am. **128**, 909 (2010).
[3] H. Autrum, Naturwissenschaften **30**, 69 (1942).
[4] G. A. Manley, Proc. Natl. Acad. Sci. U.S.A. **97**, 11736 (2000).
[5] M. R. Szpir, S. Sento, and D. K. Ryugo, J. Comp. Neurol. **295**, 530 (1990).
[6] M. Jørgensen, B. Schmitz, and J. Christensen-Dalsgaard, J. Comp. Physiol. A **168**, 223 (1991).
[7] J. Christensen-Dalsgaard and C. E. Carr, Brain Res. Bull. **75**, 365 (2008).
[8] J. W. Schnupp and C. E. Carr, Nat. Neurosci. **12**, 692 (2009).
[9] J. Christensen-Dalsgaard, Y. Tang, and C. E. Carr, J. Neurophysiol. **105**, 1992 (2011).
[10] S. N. Rschevkin, *A Course of Lectures on the Theory of Sound* (Pergamon, Oxford, 1963), p. 111.
[11] S. Temkin, *Elements of Acoustics* (Wiley, New York, 1981).
[12] N. H. Fletcher, *Acoustic Systems in Biology* (Oxford University Press, Oxford, 1992).
[13] G. A. Manley, J. Comp. Physiol. **81**, 239 (1972).
[14] See D. Heider, A. P. Vedurmudi, and J. L. van Hemmen (TUM) for a mathematical justification.
[15] J. Christensen-Dalsgaard and G. A. Manley, J. Assoc. Res. Otolaryngol. **9**, 407 (2008).